Single-Molecule Resonance Energy Transfer and Fluorescence Correlation Spectroscopy of Calmodulin in Solution†

Brian D. Slaughter, Michael W. Allen, Jay R. Unruh, Ramona J. Bieber Urbauer,‡ and Carey K. Johnson*

Department of Chemistry, 1251 Wescoe Hall Drive, University of Kansas, Lawrence, Kansas 66045-7582

Received: February 4, 2004; In Final Form: April 13, 2004

Calmodulin is a calcium-signaling protein that is involved in a diverse range of biological pathways. The flexibility of the two lobes of CaM about a central linker domain is crucial to target recognition and binding. We have attached fluorescent probes to the N-terminal and C-terminal domains of CaM. In this study, we report single-molecule Förster resonance energy transfer (FRET) between the two domains. We have detected fluctuations in single-molecule FRET efficiency on the microsecond and millisecond time scales by fluorescence correlation spectroscopy (FCS). The cross-correlation decay due to FRET on the 100 μs time scale is sensitive to the Ca^{2+} concentration, with similar relaxation at a saturating Ca^{2+} concentration of 100 μM and in the absence of Ca^{2+}, but distinctly slower relaxation in the presence of 1 μM Ca^{2+}. We have also measured the FRET efficiency distribution by analysis of fluorescence bursts in solution. The distributions of single-molecule FRET efficiencies reveal the existence of multiple conformations in solution. At least two distinct conformations are detected and attributed to distinct configurations of the N- and C-terminal domains about the central linker of CaM. These distributions are confirmed by time-resolved ensemble FRET measurements. In addition, FCS yields the diffusion coefficient for CaM. We discuss in detail issues involved in analysis of single-molecule FRET measurements, including analysis of signals and the nature and effect of dye interactions with the protein.

Introduction

Calmodulin (CaM) is a calcium-signaling protein that is involved in many biological signaling pathways, including Ca^{2+} transport and muscle contraction.[1] CaM is a small (148 amino acids) protein with two globular domains connected by an extended linker.[2−4] CaM binds four Ca^{2+} ions in response to an increase in intracellular Ca^{2+} levels, two each in the N-terminal and C-terminal lobes.[5,6] Upon binding Ca^{2+}, CaM adopts a structure that makes hydrophobic regions available for target binding.[7] Structures of apoCaM and Ca^{2+}−CaM are shown in Figure 1. CaM activates a diverse range of target enzymes, many of which share little sequence homology.[8] The central linker is known to be highly flexible in both the Ca^{2+}-loaded and Ca^{2+}-free (apoCaM) forms.[9,10] In the case of Ca^{2+}−CaM, this flexibility may be important for the ability of CaM to recognize and activate highly variable targets. Dynamic motions of CaM have been observed on time scales spanning many orders of magnitude, including nanosecond wobbling motion,[11,12] motions about the central helix on the microsecond and millisecond time scales,[13,14] Ca^{2+} binding dynamics on the millisecond time scale,[15,16] and target binding on a time scale that may span seconds to many minutes.[17]

Several structures have been reported for Ca^{2+}−CaM and apoCaM. The first crystal structures for Ca^{2+}−CaM showed an extended central helix between the N-terminal and C-terminal lobes.[3] However, the structure of CaM in solution is slightly less extended.[12,18,19] In contrast, a recent crystal structure reports a compact structure of Ca^{2+}−CaM with the opposing lobes in close proximity.[20] NMR structures predict a bent central linker for apoCaM, with opposing lobes separated by less than 40 Å.[4,7] Multiple stable conformations of both Ca^{2+}−CaM and apoCaM have been observed by fluorescence spectroscopy[18] and NMR.[10,21] In their determination of the crystal structure of Ca^{2+}−CaM, Wilson and Brunger found a high degree of structural plasticity, leading them to conclude that a number of conformational states of CaM exist and that motion between substates could be a factor in the ability of CaM to interact with diverse targets.[22] However, the presence of conformational substates and the time scale of interconversion between substates have been difficult to verify and characterize by conventional ensemble techniques.

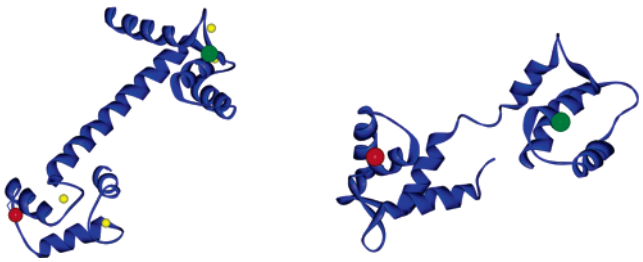

Figure 1. Structures of Ca^{2+}−CaM (left, pdb 1cll[3]) and apoCaM (right, pdb 1cfd[4]). Red and green spheres represent sites of attachment of probes Alexa Fluor 488 and Texas red. In the case of Ca^{2+}−CaM, yellow spheres represent Ca^{2+}.

Single-molecule spectroscopy has the capability to resolve minority populations and to determine the dynamics and

† Part of the special issue "Gerald Small Festschrift".

* Corresponding author. Phone: 785-864-4219. Fax: 785-864-5396. E-mail: ckjohnson@ku.ed.

‡ Current address: Department of Biochemistry and Molecular Biology, University of Georgia, Athens, Georgia.

10.1021/jp040098u CCC: $27.50
Published on Web 06/11/2004

heterogeneity of motion for diverse biological systems.[23,24] The suggested conformational flexibility of CaM and the wide range of time scales reported for exchange by NMR studies[10,14,21] make CaM well suited for study by single-molecule spectroscopy in order to answer questions about the conformations of CaM that are present in solution and the time scale of interconversion between these states.

One of the potentially most powerful single-molecule techniques is Förster resonance energy transfer (FRET),[25,26] which involves the distance-dependent nonradiative energy transfer from a donor fluorophore to an acceptor fluorophore. FRET has recently been applied on the single-molecule level to a number of protein and DNA systems.[27−34] Previous single-molecule FRET measurements on a CaM−cameleon protein construct by Moerner and co-workers revealed FRET fluctuations and Ca^{2+}-dependent FRET distributions on the millisecond time scale.[35] The power of single-molecule FRET lies in its ability to uncover multiple conformations and to determine the time scales of dynamic events involved in the function of a biomolecule. FRET can be combined with another powerful single-molecule technique, fluorescence correlation spectroscopy (FCS),[36,37] to probe the conformations and dynamics of molecules diffusing freely in solution. FCS has been used to determine a range of properties of molecules in solution, such as diffusion coefficients, triplet blinking kinetics, and protein dynamics for freely diffusing biomolecules.[38−42] FCS FRET was recently applied to a CaM−cameleon protein construct in solution in the laboratory of Gratton and co-workers, who detected fluctuations on the time scale of tens of microseconds.[43]

In this paper we combine single-molecule FRET with FCS and fluorescence burst analysis to probe the dynamics and conformational distributions of CaM in solution. We demonstrate here the capability to resolve dynamics on the microsecond and millisecond time scales and detect fluctuations in FRET efficiency for Ca^{2+}−CaM and apoCaM. The FRET efficiency distributions also reveal the presence of distinct conformations of CaM in solution. In the analysis of single-molecule FRET measurements, it is important to take into account the interaction of the fluorescent dyes with the protein. We have measured the time-resolved fluorescence and anisotropy decays of each dye at each labeling site to understand the nature of these interactions.

Experimental Methods

Sample Preparation. CaM T34/110C was expressed, purified, fluorescently labeled, and separated following methods described previously.[44] Briefly, threonine residues 34 and 110 of chicken CaM (CaM T34/110C) were mutated to cysteines using a PCR method previously described.[45,46] The expression vector of CaM T34/110C was inoculated in *E. coli* and grown in a standard M9 medium. The culture was harvested, and the CaM mutant was purified using a Phenyl Sepharose CL-4B resin. The purified CaM T34/110C was labeled simultaneously with Alexa Fluor 488 maleimide (AF488) and Texas red maleimide (TR). The double-labeled construct (CaM−DA) was separated using reverse phase HPLC and a C5 Bio Wide Pore column. A CaM−T34C construct was labeled with AF488 or TR, and free dye was removed by gel filtration or extensive dialysis. Expression, purification, and labeling of CaM−T110C were carried out by methods similar to those for CaM−T34C.

Experimental Setup. Buffer conditions for the Ca^{2+}-loaded experiments with CaM consisted of 10 mM HEPES, pH 7.4, 0.1 M KCl, 1 mM $MgCl_2$, 0.1 mM $CaCl_2$. For studies with apoCaM, CaM−DA was diluted using 10 mM HEPES, pH 7.4, 0.1 M KCl, 1 mM EGTA. These conditions led to a free Ca^{2+} concentration of less than 40 nM. For studies of CaM−DA at intermediate Ca^{2+} levels, buffer conditions were 10 mM HEPES, pH 7.4, 0.1M KCl, 1 mM $MgCl_2$, 0.1 mM $CaCl_2$, and 105 mM EGTA, leading to free Ca^{2+} levels of around 1 μM. Sucrose buffers A and B were identical to the high Ca^{2+} buffer but with 12% sucrose by weight for the sucrose A solution and 29% sucrose by weight for the sucrose B solution. These buffers correspond to viscosities of 1.4 and 3.1 cP, respectively. CaM−DA concentrations were on the order of 100 pM.

The 488 nm line of an Ar^+/Kr^+ laser (Lexel) was directed into an inverted fluorescence microscope (Nikon TE2000) and reflected with a dichroic mirror (Q505LP, Chroma Technologies) onto a 1.3 NA, 100× oil-immersion objective (SuperFluor). The objective focused the laser light onto the sample and then collected the fluorescence emission. The excitation power was 60 μW. The emission passed through the same dichroic mirror and was sent out the side port of the microscope. Outside of the microscope, a dichroic filter (565DCLP, Chroma Technologies) was used to separate the donor and acceptor fluorescence emission. Band-pass filters were placed in front of the donor (HQ525/50M, Chroma Technologies) and acceptor (HQ620/75M, Chroma Technologies) channel detectors. Single-photon counting avalanche photodiodes (SPCM-ARQ-14, Perkin-Elmer) were used to count the fluorescence photons.

Fluorescence Correlation Spectroscopy. A drop (20−30 μL) of CaM−T34C−AF488 (typically around 300 pM) in the appropriate buffer was placed on a microscope slide on top of the microscope. The microscope objective was focused a minimum of 20 μm above the surface of the microscope slide. At this focus, fluorescence from molecules that adhere to the glass surface is rejected by the confocal setup. Fluorescence trajectories were obtained with counts binned in 5 μs time intervals. Fluorescence counts were autocorrelated according to

$$G(\tau) = \frac{\langle \delta I(t)\, \delta I(t+\tau)\rangle}{\langle \delta I(t)^2\rangle} \tag{1}$$

where

$$\delta I(t) = I(t) - \langle I(t)\rangle \tag{2}$$

and I represents the fluorescence counts in a bin. The autocorrelations were fit according to[47]

$$G(\tau) = \left[\frac{1}{a}\left(w\left(\frac{1}{1+\tau/\tau_{D1}}\right)\left(\frac{1}{(1+(K_1)\tau/\tau_{D1})}\right)^{1/2} + (1-w)\left(\frac{1}{1+\tau/\tau_{D2}}\right)\left(\frac{1}{(1+(K_2)\tau/\tau_{D2})}\right)^{1/2}\right)\right] \tag{3}$$

where τ_{D1} and τ_{D2} represent transit times for a single species, and

$$K_1 = \left(\frac{r_1}{z_1}\right)^2 \qquad K_2 = \left(\frac{r_2}{z_2}\right)^2 \tag{4}$$

The variables r_i and z_i in eq 4 represent the lateral and axial half-lengths of each component of the excitation profile, which in this experiment can be adequately fit by diffusion through two three-dimensional Gaussian profiles. The diffusive dynamics cannot adequately be described by a single diffusion time through a Gaussian focal region due to a relatively large aperture (see the Results and Discussion).

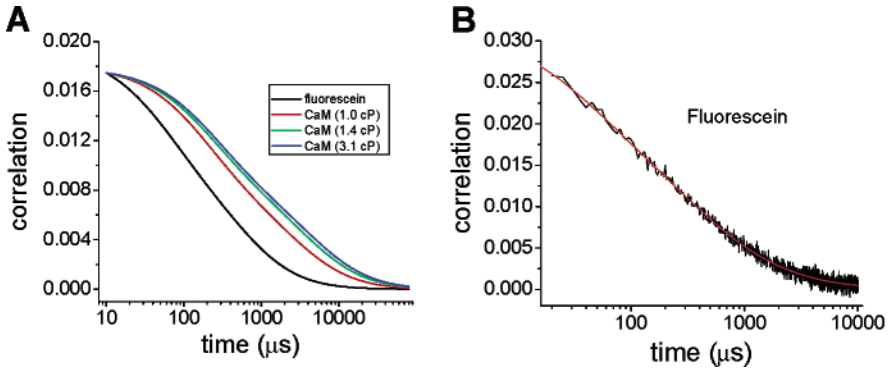

Figure 2. (A) Fits of multiple autocorrelations for fluorescein and CaM−T34C−AF488 as a function of viscosity. (B) Example of raw data and the corresponding fit to eq 3.

Cross-Correlation Analysis. For FCS cross-correlation analysis, donor and acceptor fluorescence counts were collected in 5 μs bins and fluorescence counts were cross correlated. The cross-correlation curve includes decay due to diffusion and is fit by

$$G(\tau) = \left[\frac{1}{a}\left(w\left(\frac{1}{1+\tau/\tau_{D1}}\right)\left(\frac{1}{(1+(K_1)\tau/\tau_{D1})}\right)^{1/2} + (1-w)\left(\frac{1}{1+\tau/\tau_{D2}}\right)\left(\frac{1}{(1+(K_2)\tau/\tau_{D2})}\right)^{1/2}\right)(E(\tau))\right] \quad (5)$$

where $E(\tau)$ describes the time dependence of the cross correlation due to FRET (see the Results and Discussion).

Analysis of FRET Distributions. FRET efficiencies were determined in 75 μs or 800 μs bins. The FRET efficiency for each time bin is given by

$$E = \frac{cI_a}{cI_a + I_d} \quad (6)$$

where c is a factor to correct for the relative detection efficiency of the donor and acceptor channels. Ensemble fluorescence lifetime measurements of CaM−DA were also carried out. The FRET efficiency can also be determined from the fluorescence lifetime:

$$E = 1 - \frac{\tau_{DAi}}{\tau_D} \quad (7)$$

where τ_D is the fluorescence lifetime of the donor-only labeled construct and τ_{DAi} is the ith donor fluorescence decay component of CaM−DA.[48] From the FRET efficiency, distances (R) can be obtained according to

$$R = \left(\frac{1-E}{E}\right)^{1/6} R_0 \quad (8)$$

where R_0 is the Förster distance, or distance of 50% energy transfer between donor and acceptor. For AF488 and TR, a distance of 46.5 Å was calculated from the spectral overlap of the donor fluorescence and acceptor absorption.[48]

Time-Resolved Fluorescence. Time-resolved fluorescence spectroscopy was carried out by time-correlated single-photon counting (TCSPC) with an instrument that has been described previously.[49] Briefly, for excitation of TR, a mode-locked, frequency-doubled Nd:YAG laser (Coherent Antares) synchronously pumped a home-built rhodamine 6G dye laser operated at 590 nm and cavity-dumped at 3.8 MHz. For excitation of AF488, a 440 nm picosecond pulsed diode laser (LDH 440, Picoquant GmbH) was operated at 10 MHz. The monochromator band-pass was 10 nm for all time-resolved experiments. The emission wavelength was 612 nm for TR and 512 nm for AF488. All intensity decays were collected with a polarization at 54.7° from vertical. A correction factor for the normalization of collection intensity of parallel and perpendicular anisotropy decays was obtained by comparison of integrated decay intensities with the steady-state anisotropy values. Globals Unlimited decay analysis software (Laboratory for Fluorescence Dynamics, University of Illinois at Urbana-Champaign) was used for data analysis. The fit to the decays was convoluted with an instrument response function collected using scatter from a solution of nondairy creamer. The support-plane method was used to obtain estimates of error limits at one standard deviation.[48,50] FRET distributions were determined from time-resolved fluorescence decays of CaM−DA by fitting to Gaussian distributions of lifetimes or by fitting with a maximum entropy algorithm.[51]

Results and Discussion

Determination of Translational Diffusion Coefficients. The translational diffusion coefficient of CaM has been measured previously by a number of techniques, including fluorescence recovery after photobleaching (FRAP),[52] gel electrophoresis,[53] and molecular dynamics simulations.[19,54] As FCS has become a valuable technique for monitoring diffusion and dynamics of biomolecules,[55,56] it is useful to compare diffusion coefficients measured by FCS with previous measurements obtained by other techniques. The autocorrelation decays of CaM−T34C−AF488 were also used to obtain the parameters τ_{D1}, τ_{D2}, w, K_1, and K_2 in eq 3 for use in fits of cross correlations of donor and acceptor fluorescence counts from CaM−DA. This entails the reasonable assumption that the translational diffusion coefficient for double-labeled CaM is the same as that for single-labeled CaM.

Fits of FCS autocorrelations for fluorescein and CaM−T34C−AF488 at varying viscosities are shown in Figure 2A. Raw data and the corresponding fit for Ca^{2+}−CaM at a viscosity of 1.0 cP are shown in Figure 2B. The autocorrelation decays could not be fit with a single transit time; rather, two were required (eq 3). Diffusion coefficients of CaM were determined from the fast and slow transit times (τ_{D1} and τ_{D2}) by the relation

$$D = \frac{r_0^2}{4\tau_{Di}} \quad (9)$$

after calibration with the known diffusion coefficient of fluorescein ($D = 3.2 \times 10^{-6}$ cm^2/s at 25 °C).[57,58] Diffusion coefficients of Ca^{2+}−CaM−T34C−AF488 as a function of viscosity were obtained relative to fluorescein and are listed in

TABLE 1: Transit Times and Diffusion Coefficients for CaM as a Function of Viscosity

	τ_{D1} (μs)	D (10^{-7} cm^2/s)[a]	τ_{D2} (μs)	D (10^{-7} cm^2/s)[a]
fluorescein[b]	46	32	421	32
CaM−DA, 1.0 cP	174	7.8	2066	6.5
CaM−DA, 1.4 cP	212	6.4	3126	4.3
CaM−DA, 3.1 cP	259	5.2	3944	3.4

[a] Uncertainties in the mean for the diffusion coefficients, found by fitting of multiple data sets, are on the order of 0.2−0.4 × 10^{-7} cm^2/s. [b] The diffusion coefficient of fluorescein is taken from refs 57 and 58.

Table 1. For CaM, the fast transit time τ_{D1} is on the order of a few hundred microseconds and the slow transit time τ_{D2} is on the order of several milliseconds. Multiple transit times for a single species have been reported previously and attributed either to saturation of the fluorophore at the high-intensity center of the focal region or to the use of a large aperture, which allows fluorescence from the "wings" of the excitation profile to reach the detector.[47,59] We observed no power dependence in fits with two transit times in the current study; thus, it is likely that the necessity for two diffusion terms is a result of the relatively large aperture (the active area of the avalanche photodiode).

The observation of two transit times of at least an order of magnitude apart is of interest, as dye transit times ranging from 40 μs to over 1 ms have been reported for similar microscope systems.[38,60] As pointed out previously[61] and shown by the current results, it is possible to resolve multiple transit times for a single species, though the short time might be misinterpreted or missed altogether, depending on the size of the time bin used in an experiment The techniques of FRET analysis used in this study report on relative donor and acceptor counts and thus are unaffected by whether the molecule of interest is being excited in the center of the excitation profile or the wings. Therefore, the presence of the long transit time that is observed in the autocorrelation decays is a significant advantage for probing dynamics because it expands the observation time of freely diffusing CaM to a range of several milliseconds.

The diffusion coefficient of fluorescein in water is 3.2 × 10^{-6} cm^2/s at 25 °C.[57,58] The fit of the average of multiple autocorrelations of fluorescein to eq 3 yields transit times of 46 μs and 420 μs and values of K_1 and K_2 of 0.426 and 0.0604, respectively. The small value of K_2 relative to that of K_1 reflects contributions from fluorescence emitted by molecules displaced in the z direction from the focal plane. The different values of the ratio of longitudinal and axial half-lengths for the short and long diffusion components were not taken into account by previous workers, who assumed a single ratio of lateral to axial half-lengths ($K_1 = K_2$). Use of the published diffusion coefficient of fluorescein allows the calculation of $r_1 = 230$ nm (eq 4) from the transit time. The half-length for axial resolution can then be calculated ($z_1 = 360$ nm). These values are in close agreement with profile parameters obtained in other studies using similar objective lenses.[47,60,62] Similarly, use of the slow transit time of fluorescein with K_2 yields $r_2 = 730$ nm and $z_2 = 3.0$ μm. As all data for the determination of diffusion coefficients was obtained with an identical experimental setup, K_1 and K_2 in the fits of the autocorrelations of CaM were fixed to the values determined with fluorescein.

The fast transit time of Ca^{2+}−CaM with the calibrated longitudinal half-length r_1 yields a diffusion coefficient for Ca^{2+}−CaM of 7.8 × 10^{-7} cm^2/s (see Table 1). In a similar manner, use of r_2 with the slow transit time of CaM yields a similar diffusion coefficient of 6.5 × 10^{-7} cm^2/s. No significant change in diffusion coefficient as a function of Ca^{2+} concentration was observed. These values agree well with the diffusion coefficient of 6.1 × 10^{-7} cm^2/s, which can be calculated from the transit time of 250 μs that was determined for CaM in solution measured in a two-photon FCS measurement.[63] The diffusion coefficients measured here are also in good agreement with molecular dynamics simulations conducted by Kuczera and co-workers, who report diffusion coefficients of 7 ± 1 × 10^{-7} cm^2/s and 6 ± 3 × 10^{-7} cm^2/s for apoCaM and Ca^{2+}−CaM, respectively.[19,54] The diffusion coefficients observed here are also consistent with, though slightly lower than, those found by fluorescence recovery after photobleaching (FRAP) (1.02 ± 0.13 × 10^{-6} cm^2/s)[52] and gel electrophoresis (9.2 × 10^{-7} cm^2/s).[53]

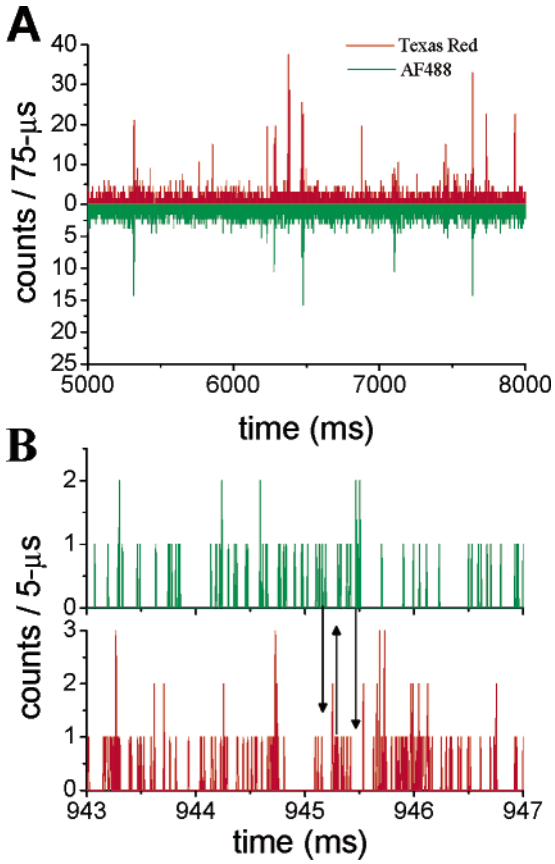

Figure 3. (A) Examples of fluorescence bursts obtained with 75 μs bins, with donor (AF488) in green and acceptor (Texas red) in red. Acceptor counts are not observed due to direct excitation and are thus evidence of high FRET efficiency. (B) Donor and acceptor counts in 5 μs bins for a region of high signal. Arrows are to emphasize areas of cross correlation.

The dependence of the diffusion coefficient on viscosity is shown in Table 1. The diffusion coefficients decrease with viscosity as expected in 12% by weight sucrose buffer, but the apparent decrease in the diffusion coefficient is less than expected in the 29% w/w sucrose buffer. This is particularly apparent for the diffusion coefficients determined from the short transit time, possibly because of increased photobleaching for the CaM−AF488 molecules at high viscosity as the time in the focal volume is lengthened.

Analysis of FRET Signals. Fluorescence bursts were detected as CaM−DA molecules traversed the focal volume. Examples of bursts of CaM−DA excited at 488 nm with 75 μs bins are shown in Figure 3A. In control experiments, single-molecule bursts could not be detected from CaM−T34C labeled only with TR upon excitation at 488 nm. Thus bins with high count levels in the acceptor channel are evidence of high FRET efficiency.

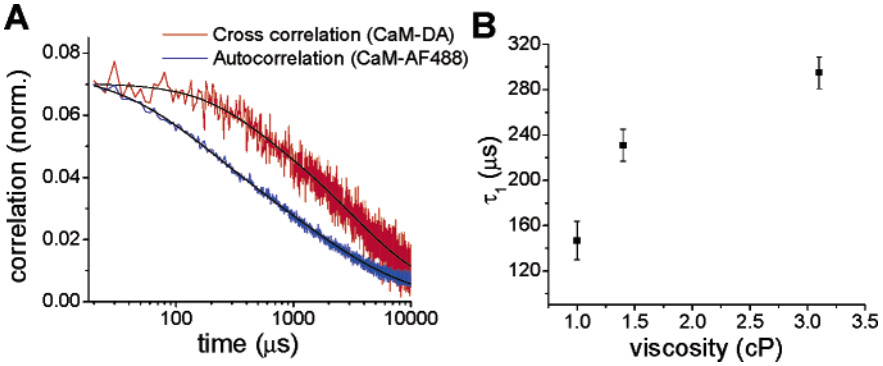

Figure 4. (A) Fit of cross correlation of CaM−DA according to eqs 5 and 10 compared to the autocorrelation decay of CaM−AF488 at a viscosity of 1.0 cP. Data were obtained in 5 μs bins. (B) Dependence of the fast fluctuation correlation time constants on viscosity from the fits of the cross correlations to eqs 5 and 10.

An example of a fluorescence trajectory recorded in 5 μs bins in donor and acceptor channels is shown in Figure 3B. At this bin length, most bins contain zero or one count, with occasional cases of two or three counts in a bin. Several examples of areas of anticorrelation between donor and acceptor fluorescence are noted with arrows in Figure 3B. These areas are evidence of fluctuations in FRET efficiency.

In order to analyze the fluctuations in FRET efficiency, we calculated the cross-correlation function between donor and acceptor fluorescence signals. Emission from codiffusing fluorophores AF488 and TR attached to the same CaM molecule leads to a positive cross-correlation function between donor and acceptor channels.[64,65] The existence of fluctuations in FRET efficiency between probes is signaled by an anticorrelated contribution to the cross-correlation function. The time dependence of the cross-correlation function can thus reveal time scales of motion between donor and acceptor probes. Cross-correlation functions were calculated by direct cross correlation of the donor and acceptor fluorescence counts obtained in 5 μs bins. A cross-correlation curve obtained in this way is shown in Figure 4. In the absence of FRET, the cross-correlation decays would be dominated by diffusion and would resemble the decays in Figure 2A. The strong anticorrelation of donor and acceptor counts generates a rising contribution to the cross-correlation curve shown in Figure 4.

In order to resolve the contribution of FRET to the cross-correlation curves, the component of the curves due to diffusion must first be known. In order to account for diffusion in the cross-correlation curve, the decay parameters τ_{D1}, τ_{D2}, w, K_1, and K_2 in eq 5 were fixed to the values determined from the fit of diffusion of CaM−T34C−AF488. Upon inspection of Figure 4A the rise in the cross-correlation curve relative to the autocorrelation curves is manifested as a flattening in the decay curve. Visual comparison of the autocorrelation decay of CaM−T34C−AF488 and the cross-correlation decay of CaM−DA in Figure 4A shows the presence of FRET dynamics on the 100 μs to 1 ms time scale. This component is accounted for by the factor $E(\tau)$ in eq 5. We found that it was not possible to fit the rise in the cross-correlation function to a single time constant, but it could be fit with two time constants τ_{F1} and τ_{F2}:

$$E(\tau) = (1 - f\,e^{-\tau/\tau_{F1}} - g\,e^{-\tau/\tau_{F2}}) \qquad (10)$$

An example of a measured cross-correlation function with the corresponding fit for Ca^{2+}−CaM−DA is shown in Figure 4A next to the autocorrelation of CaM−T34C−AF488. The time constants for the decay of anticorrelation as a function of viscosity are tabulated in Table 2. Figure 4B plots the anticorrelation time constant τ_{F1} (eq 10) as a function of viscosity.

TABLE 2: FRET Time Constants for CaM as a Function of Ca^{2+} and Viscosity

		FCS-cc (5 μs bins)	
		τ_{F1} (μs)	τ_{F2} (ms)
1.0 cP	<40 nM	172 ± 19	5 ± 2
	~1.0 μM	364 ± 23	45 ± 16
	100 μM	147 ± 17	2 ± 5
1.4 cP	100 μM	231 ± 14	30 ± 19
3.1 cP	100 μM	295 ± 14	81 ± 44

Dynamics of Fluorescently Labeled CaM. Comparison of cross correlations of CaM at three Ca^{2+} levels reveals a Ca^{2+} dependence in the time scale of the motions that underlie the anticorrelation between donor and acceptor. The cross correlations with 5 μs bins yielded fast time constants of 147 ± 17 μs for Ca^{2+}−CaM and 172 ± 19 μs for apoCaM. However, cross correlations of CaM−DA at an intermediate Ca^{2+} level (~1.0 μM) yielded longer time constants of 364 ± 23 μs. These results could have important implications for target binding. Motions of CaM on this time scale may contribute to the ability of CaM to activate diverse targets, in that rapid domain motions may increase the probability of exploring a favorable conformation for binding during the time that CaM and the target are in close proximity. The longer time constant at an intermediate Ca^{2+} concentration may indicate altered dynamics when the Ca^{2+} binding sites are only partially occupied. The cross correlations in Figure 4A do not decay to zero on the time scale of the burst length, which can range up to many milliseconds in the high-viscosity solutions, but instead the long time constants range up to tens of milliseconds. This shows that anticorrelation between donor and acceptor channels persists past the time range of the fluorescence bursts from freely diffusing CaM, although it is not possible to accurately resolve dynamics on a time scale longer than the average transit time for a single molecule. The observation of dynamics on the millisecond time scale is not surprising, because dynamics of CaM are known to extend out to the time scale of milliseconds, as observed by single-molecule FRET by Moerner and co-workers.[35]

Several control experiments were carried out in an effort to understand the origin of the microsecond time-scale dynamics observed by single-molecule FRET in CaM−DA. One potential source of fluctuations in energy transfer efficiency could be triplet kinetics associated with intersystem crossing of the acceptor. Autocorrelation decay as a result of populating the acceptor triplet state has been observed previously in FCS on

the time scale of <5 μs for the dyes rhodamine 6G and fluorescein isothiocyanate.[39,47] In FCS experiments on CaM−T34C−TR, we observed a decay in the autocorrelation on a time scale shorter than 5 μs with 2 μs bins, suggesting that triplet dynamics affect the cross correlation on a time scale much shorter than 100 μs. As a control experiment, we directly excited CaM−T34C−TR which was immobilized in an agarose gel by fusion to maltose binding protein[44] at an excitation rate comparable to that expected from FRET in CaM−DA. An autocorrelation of the TR fluorescence revealed fluctuations for some molecules, but a component on the 100 μs time scale was absent for many molecules, contrary to expectation if triplet blinking were occurring on that time scale. The fluctuations that were occasionally observed by this method were not power dependent, again contrary to expectation for triplet kinetics.

Further controls were completed to determine if uncertainty in diffusional time constants could lead to additional uncertainty in reported FRET time constants (see eqs 5 and 10). To address this possibility, FRET time constants were obtained from fits to eq 5 using the upper and lower uncertainty limits of the diffusional time constants as parameters. The resulting FRET time constants varied by less than 3%. The reported errors in the FRET time constants more than encompass this uncertainty. Thus, the reported fluctuation times are negligibly affected by uncertainty in fitting the diffusional decay.

The dependence of the cross-correlation times on Ca^{2+} concentration further supports the interpretation of FRET fluctuations in terms of the dynamics of CaM. Although the difference between the cross-correlation times measured for apoCaM and Ca^{2+}−CaM is not larger than the estimated uncertainties in these values, the cross-correlation time for a Ca^{2+} concentration of 1 μM is significantly longer than the values measured for either apoCaM or Ca^{2+}−CaM (see Table 2). Therefore, in light of the Ca^{2+}-dependent change in correlation time, it appears likely that the observed fluctuations at 1.0 μM Ca^{2+} are a feature of CaM dynamics.

Motion of CaM on these time scales has been reported in a number of studies. NMR measurements on the C-terminal of CaM and on CaM mutants revealed conformational exchange on time scales of a few hundred microseconds that was attributed in part to CaM domains sampling between multiple substates.[13,66,67] A study of CaM at low Ca^{2+} levels revealed Ca^{2+}-dependent motion on this same time scale, as well as motion that was independent of Ca^{2+} concentration.[14] Tjandra and coworkers observed conformational exchange of the C-terminal of CaM on the time scale of 350 ± 100 μs in the absence of Ca^{2+}, with one of the conformers being favored significantly (>90%) relative to the other.[10] A number of kinetic experiments have detailed the Ca^{2+} binding and release rates of CaM.[15,68] These studies have reported Ca^{2+} off rates in the range of a few milliseconds for the N-terminal of CaM and a few hundred milliseconds from the C-terminal. Ca^{2+} binding may occur much more rapidly, on the time scale of tens of microseconds to the N-terminal domain and a few milliseconds to the C-terminal domain at a Ca^{2+} concentration of 100 μM.[15] Thus a number of processes of CaM, both Ca^{2+}-dependent and Ca^{2+}-independent, appear to occur on the time scale of microseconds to milliseconds. The ability to detect and characterize FRET efficiency fluctuations between fluorescence probes on opposing lobes of CaM and to determine correlation times of the dynamics on the microsecond time scale should prove important for understanding of the nature of the protein motions that are behind these dynamics.

FRET Distributions. The FRET efficiencies calculated from donor and acceptor fluorescence signals in each bin during a fluorescence burst yield the single-molecule distribution of FRET efficiencies for a given bin size. Figure 5 shows the distributions of effective donor−acceptor distances calculated for CaM−DA from the measured FRET efficiency distributions with 75 μs and 800 μs bins. The calculated distances are termed "effective" because counting noise and potential contributions from blinking of the acceptor dye broaden the distributions. These factors are discussed in greater detail below. Uncertainties in R values due to Poisson noise are estimated to contribute on the order of a few angstroms to the width of the distributions.

In order to exclude time bins where no fluorescence signal was present in the focal volume, a signal-to-background threshold was imposed. Only signals that exceeded the threshold were included in the FRET efficiency or distance distributions. A similar approach has been taken by other workers.[29,30,42,69,70] The choice of threshold value below which it is assumed that there is no fluorophore in the focal volume can have a significant effect on the shape of the distribution that is obtained. Cutoffs can be set a number of different ways. A common approach is to set a threshold that the sum of the donor and acceptor counts must exceed to be included in the FRET distribution.[30,32,33] Another approach is to require a minimum number of counts in both the donor and acceptor channels separately. A third possibility is to include only bins that have counts that are a number of standard deviations above the background count level.[70] We computed distributions with a number of different cutoff methods. The requirement of a minimum number of counts in donor and acceptor channels separately narrowed the distribution and led to a distribution that fit well to a single Gaussian function, nearly completely missing the component of the distribution in Figure 5 that has a distance larger than 48 Å. Similarly, the requirement that the sum of counts in donor and acceptor channels exceed a set threshold in addition to the requirement that the donor and acceptor channels individually exceed a threshold proved to narrow the distributions excessively, removing regions of very high or very low FRET efficiency. Thus, the choice of threshold values and the method of excluding bins for times when no fluorophore is thought to be present in the focal volume can seriously impact the calculated distribution and may result in incorrect distributions.

The method of cutoffs implemented by Grunwell et al. was used to take into account differences in background levels in the two channels.[70] Bins with counts that were above 8 times the standard deviation of the background signal in either the donor or acceptor channel, or above 6 times the standard deviation of the sum of donor and acceptor channels were included in the distance distributions. A minimum acceptor count total of 2 times background was also required to minimize inclusion of bins that could be biased toward low FRET efficiency due to acceptor photobleaching. Control experiments were carried out to verify that excitation at 488 nm at the intensities used does not lead to significant fluorescence in the acceptor channel due to direct excitation of TR. Therefore, bins containing high acceptor counts and low donor counts can confidently be attributed to high FRET efficiency. This approach yielded the distributions in Figure 5.

For comparison with the single-molecule FRET distributions, we carried out an ensemble time-resolved fluorescence measurement on CaM−DA. These decays were fit to determine the fluorescence lifetime distributions shown in Figure 6. Although the fluorescence decay of CaM−T34C and CaM−T110C singly labeled with AF488 is single exponential, the decay of AF488

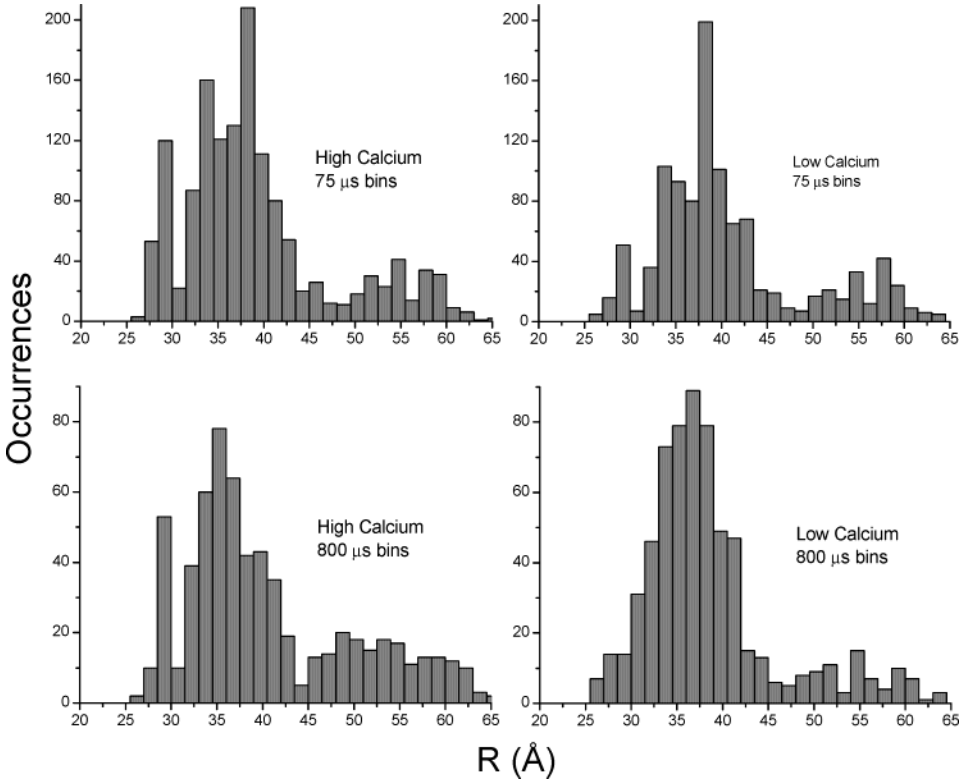

Figure 5. Distributions of CaM−DA at high and low calcium levels using 75 and 800 μs bins. Bins containing donor or acceptor counts that were 8 times above the standard deviation of the background signal, or 6 times above the standard deviation of the average sum of donor and acceptor counts, were included.

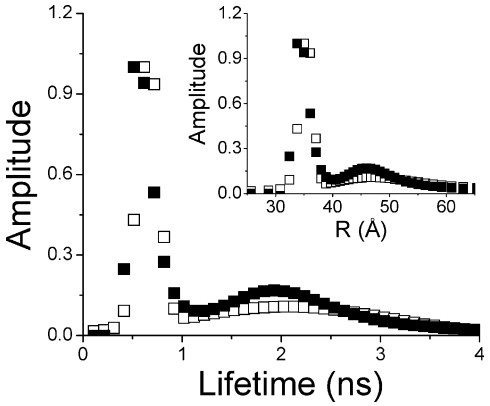

Figure 6. Time-resolved fluorescence lifetime distributions at saturating Ca^{2+} (100 μM) obtained using maximum entropy (■) and global fitting algorithms (□). In the inset is the calculated *R* distribution using an R_0 of 46.5 Å.

in CaM−DA shows two components with time constants of 2.90 ± 0.07 ns and 810 ± 40 ps. These lifetimes correspond to FRET efficiencies of 0.28 (R = 54 Å) and 0.80 (R = 37 Å). Distributions from the bulk FRET data were determined both by a fit to Gaussian lifetime distributions and by maximum entropy analysis. The corresponding distance distributions are shown in the inset. These distributions confirm the presence of multiple FRET conformations. Gaussian and maximum entropy fits both predict two distributions with nearly equal amplitudes, with slightly higher FRET efficiency than the fit to two discrete lifetimes. Globals predicts two distributions centered at lifetimes of 610 ps (35 Å) and 2.03 ns (47 Å), while maximum entropy analysis centers the distributions at 510 ps (34 Å) and 1.93 ns (46 Å). It is important to note that the distributions obtained from the single-molecule bursts match closely the distributions obtained from the bulk measurements using donor lifetimes.

Conformations of Fluorescently Labeled CaM. Distance distributions were obtained for CaM at Ca^{2+} concentrations of 100 μM and <40 nM (Figure 5). The distributions are shifted slightly to longer distance in the absence of Ca^{2+}. The average distance between donor and acceptor fluorophores obtained from these distributions is 39.6 ± 0.3 Å in apoCaM and 37.1 ± 0.3 Å in Ca^{2+}−CaM. (The uncertainties cited are the standard deviations in the mean of the distributions.) The average distances reported here between probes on the 34 and 110 sites are in general agreement with previous results. A FRET study conducted by Török and co-workers using CaM labeled at sites 34 and 110 with the probes AEDANS and DDP reported distances of 40 Å (75%) and 28 Å (25%) for Ca^{2+}−CaM and 38.9 Å for apoCaM.[18] These distances are similar to the observed distances for the present study and also show a slightly longer average distance in the apo form. The shorter distance observed between the labeling sites upon Ca^{2+} binding is consistent with a study by Squier and co-workers, who report a distance decrease of about 4−6 Å between a chromophore at residue 27 and an engineered nitrotyrosine residue at position 139 upon Ca^{2+} binding.[12] The distances for apoCaM are slightly larger than the distance of ≈35 Å predicted by the NMR structure,[4] but in the case of Ca^{2+}−CaM the experimental distance is much smaller than the crystal structure prediction of ≈53 Å.[2,3] This is consistent with the presence of a flexible linker domain for CaM in solution, rather than the rigid central helix observed in the crystal structure. It is worth noting the presence of a shoulder centered at a distance of ≈55 Å in the distance distributions (see discussion below), which may correspond to the extended conformation present in the crystal.

The distributions suggest that multiple conformations of CaM are present on the microsecond time scale. The single-molecule distributions show the presence of two or three conformations having different distances between donor and acceptor dyes,

TABLE 3: Lifetimes and Time-Resolved and Steady-State Anisotropies of Single-Labeled CaM Species at 100 μM Ca^{2+}

	τ (ns)	r_{ss}	a_1	τ_{r1} (ns)	a_2	τ_{r2} (ns)
CaM−T34C−AF488	4.13 ± 0.02	0.12 ± 0.01	0.72 ± 0.20	1.5 ± 0.4	0.28 ± 0.20	$14^{+\infty}_{-8}$
CaM−T110C−AF488	3.88 ± 0.04	0.11 ± 0.01	0.70 ± 0.10	1.0 ± 0.2	0.30 ± 0.10	12^{+3}_{-5}
CaM−T34C−TR	4.73 ± 0.02	0.23 ± 0.01	0.40 ± 0.15	2.4 ± 0.8	0.60 ± 0.15	$14^{+1}_{-0.3}$
CaM−T110C−TR	4.76 ± 0.01	0.23 ± 0.01	0.30 ± 0.25	3.1 ± 1.5	0.70 ± 0.25	11^{+7}_{-2}

with distributions centered at 36 and 55 Å for Ca^{2+}−CaM and 38 and 55 Å for apoCaM. The dominant conformation is peaked at a distance of about 37 Å in both Ca^{2+}−CaM and apoCaM. A conformation with a longer distance of about 55 Å carries about 15% of the population. A third conformation may also be present with a distance centered around 28 Å. This compact state appears much more prevalent in Ca^{2+}−CaM, with 17% of the bursts in Ca^{2+}−CaM at distances smaller than 30 Å, compared to only 9% for apoCaM.

To answer the question of how dye conformations and orientational effects might contribute to the observed conformations, we measured the time-dependent fluorescence intensity and anisotropy of the dyes (Table 3). The fluorescence decays of both AF488 and TR are fit well with a single exponential, suggesting that both dyes experience a single environment. The anisotropy decays for both CaM−T34C−AF488 and CaM−T110C−AF488 show a high amplitude (from 70% to 77%) of orientational motion of the dye on a nanosecond time scale, faster than the reorientation of the respective lobes of CaM. A remaining fraction reorients with the protein. This could suggest the presence of two populations of AF488, a majority population where AF488 reorients freely with respect to the protein, and a minor population where the dye adheres to the protein. An alternative possibility is a homogeneous population of AF488 in which the motion of AF488 is partially restricted, resulting in two anisotropy decay components. This case could be described by the well-known wobbling-in-a-cone model. The single fluorescence lifetime of AF488 for both CaM−T34C−AF488 and CaM−T110C−AF488 suggests that this model is the correct one, i.e., that AF488 is free to rotate within a restricted region. In the wobbling-in-a-cone model, the anisotropy decay amplitude for the fast component predicts a cone half-angle of 49° to 53°.[71] In contrast, the anisotropy decay of CaM−T34C−TR and CaM−T110C−TR shows that TR experiences little reorientation with respect to the protein. Two anisotropy decay time constants are observed for TR. The longer of these corresponds to rotational diffusion of the protein, whereas the shorter corresponds to motion of the N-terminal or C-terminal domain. Independent orientational motion of the N- and C-terminal domains of CaM has been observed previously by several workers.[9−11] Due to the free motion of AF488 (70−77%) plus independent, nanosecond motion of the N- and C-terminal domains, it is not possible for the dye pair to adopt prolonged conformations that lead to extreme variations in κ^2 over the time scale of the time bins used. This conclusion is confirmed by the low (<15%) estimated uncertainty in κ^2 based on the measured anisotropies[72] (see below).

The distance difference of 17−18 Å between the conformations of CaM−DA with peaks at 37 Å and at 55 Å also appears to be too large to be explained by the presence of two populations of AF488, one rotating freely with respect to the protein and one stuck to it. The maximum likely distance difference between free and stuck conformations of the dye would be the length of the five-carbon linker by which the dye is attached to the cysteine residue. The maximum length of this linker is approximately 8−12 Å. A previous study that also employed AF488 with a five-carbon linker as a donor has reported a dye linkage length of 5 Å.[73] Thus, the observed distance distribution appears to correspond to conformations of CaM and not different dye conformations.

The possibility of multiple conformations of CaM has emerged in several studies based on various experimental methods. In a FRET study of Ca^{2+}−CaM using the probes AEDANS and DDP labeled at the 34 and 110 sites, Török and co-workers found that the fluorescence decay of the donor fit to two time constants corresponding to conformations where the sites are separated by 40 Å in one conformation and 28 Å in a second conformation.[18] The longer lifetime component corresponding to a more extended structure had the dominant amplitude (0.75 ± 0.15 compared to 0.25 ± 0.15). The fraction of the population in the compact structure of Ca^{2+}−CaM (17%) is consistent with the amplitude of the donor lifetime decay in the FRET experiment of Török and co-workers,[18] which was attributed to a distance of 28 Å. A recent X-ray structure of Ca^{2+}−CaM also reveals a compact structure, with sites 34 and 110 separated by less than 20 Å.[20] This is in contrast to other reported Ca^{2+}−CaM structures[2,3] that predict a more extended central helix. Although the single-molecule distributions in Figure 5 suggest the presence of a conformation at 28 Å, particularly in Ca^{2+}−CaM, we were not able to resolve a fast fluorescence decay component corresponding to the compact state centered at 28 Å in the single-molecule distributions. The resolution of such a state is more suited to the FRET system of Török and co-workers, where the dye pair has a Förster distance of about 26 Å, as opposed to the dye pair in the current study, with a Förster distance of 46.5 Å. On the other hand, a distribution centered around 55 Å is much more easily observed with the longer Förster distance and may not have been detectable with a Förster distance of 26 Å. Small-angle X-ray scattering experiments have also indicated the presence of extended conformations of CaM in solution, with maximum lengths of the protein approaching 60 Å.[74,75]

The observation of distributions with multiple conformations raises the question of the time scale over which the subpopulations interconvert. If multiple conformations are present on the time scale of the measurement, a narrowing of the distribution with an increase in bin time may yield information about the time scale of interconversion between substates. Distributions obtained using longer time bins (up to 800 μs) still show evidence of multiple conformations. This suggests that the FRET fluctuations on the 100 μs time scale cannot be attributed to interconversion among these substates. The amplitude of the extended conformation is nearly identical for Ca^{2+}−CaM (15% of bursts at R longer than 48 Å) and apoCaM (17%). There does not appear to be a significant change in the amplitude of the extended conformation with 800 μs bins, suggesting that these conformations interconvert over a longer time scale. The longer of the two time constants (on the order of milliseconds)

for FRET fluctuations may correspond to interconversion between multiple conformations; however, this cannot be demonstrated within the transit time of freely diffusing CaM in the present experiments.

One potential source of uncertainty in FRET measurements is the value of the orientational factor κ^2 in the calculation of the Förster radius R_0. In the present study, the value of κ^2 was set equal to $^2/_3$, the value for averaging over all relative orientations of donor and acceptor. Experimental and theoretical considerations suggest that uncertainty in κ^2 does not significantly influence the calculated distances in this study. One way to evaluate the uncertainty in the value of κ^2 is based on the steady-state anisotropies of the donor and acceptor dyes.[72,76] In the present case, the motion of TR is coupled to CaM with a steady-state anisotropy of 0.23 for both CaM−T34C−TR and CaM−T110C−TR (Table 3). In contrast, the steady-state anisotropies of CaM−T34C−AF488 and CaM−T110C−AF488 are 0.12 and 0.11, respectively, indicating orientational freedom of the dye relative to the protein. Although the anisotropy and κ^2 factors are characterized by averages over different angular functions, the steady-state anisotropies provide information limiting the range of possible values of κ^2.[76] A study reporting the error in R for donor and acceptor probes with varying polarization was conducted by Haas and co-workers.[72] On the basis of their work, the highest possible error in the determination of R due to setting κ^2 equal to $^2/_3$ in the current study is less than 15%. It should be stressed that the objective of the present study is to obtain dynamic and conformational information, not absolute distances. Even so, as discussed above, reported distances in this study match closely distances from previous studies, and the expected error due to κ^2 is low.

Conclusions

The methods presented here demonstrate the power of single-molecule FRET combined with FCS techniques to reveal dynamics on time scales relevant for the function of proteins. We have demonstrated the potential of FRET−FCS methods to detect dynamic fluctuations on the 100 μs time scale and have reported distance distributions that reveal the presence of multiple conformations in solution. However, in analyzing these findings, careful consideration of the potential role of dye interactions with the protein is required.

An important and surprising conclusion of the FRET measurements is the presence of multiple, long-lived conformations of CaM in solution. This result suggests that CaM is an example of a protein where multiple conformations are important for protein function.[77] Curiously, the predominant conformation in solution for Ca^{2+}−CaM does not correspond to any of the available crystal structures,[2,3,20] consistent with NMR results indicating a highly flexible central helix in solution.[9,21] Distributions of CaM at both Ca^{2+} levels reveal a compact conformation, with an average distance between lobes of around 36 Å for Ca^{2+}−CaM and 38 Å for apoCaM, and a second, more extended conformation centered around 55 Å, which may correspond to the conformation found in the crystal structure of Ca^{2+}−CaM. There appears to be a third distribution for Ca^{2+}−CaM with an average distance of around 28 Å, similar to one that has been observed by Török and co-workers.[18] Time-resolved FRET of Ca^{2+}−CaM−DA verified the distributions, predicting conformations with FRET efficiencies of 0.80 and 0.28 with relative amplitudes of 0.70 and 0.30, respectively.

Fluorescence correlation spectroscopy has been used to verify the translational diffusion coefficient of CaM. Values of 7.8×10^{-7} cm^2/s and 6.5×10^{-7} cm^2/s were obtained for Ca^{2+}−CaM with use of τ_{D1} and τ_{D2}, respectively. Fluorescence from molecules away from the central focal region, a result of the use of a relatively large aperture, allowed for observation of freely diffusing CaM on the time scale up to milliseconds.

Cross correlations of donor and acceptor probes attached to opposing globular domains of CaM have revealed motion on a number of time scales. Cross correlations of donor and acceptor fluorescence counts in 5 μs bins yielded FRET time constants of 147 ± 17 μs and 172 ± 19 μs for Ca^{2+}−CaM and apoCaM, respectively, and significantly longer (364 ± 23 μs) time constants at an intermediate Ca^{2+} concentration of 1 μM. The Ca^{2+} dependence of these fluctuations supports the conclusion that the dynamics on this time scale are a feature of CaM itself and not dye interactions with the protein. Fluctuations between lobes on this time scale could have important implications for target recognition and binding. A second time constant was required to fit the cross correlations. This time constant was on the order of milliseconds but was difficult to resolve with freely diffusing CaM, as it was on the same order as the transit time.

Acknowledgment. This paper is dedicated to Professor Gerald J. Small in recognition of his leadership in the field of the molecular spectroscopy of biomolecules and molecular solids, and with thanks for his mentorship and guidance. We thank Enrico Gratton and Lloyd Davis for discussions about FCS cross-correlation measurements, N. Periasamy for use of his maximum entropy fitting program, and Ken Osborn for development of in-house software used in the data analysis. We acknowledge support for this research from NIH ROI GM58715 and a Research Corporation Research Opportunity Award. B.D.S. and J.R.U. acknowledge support from the Dynamic Aspects of Chemical Biology NIH Training Grant (NIH 5 T32 GM08545-09).

References and Notes

(1) Chin, D.; Means, A. R. *Trends Cell Biol.* **2000**, *10*, 322−328.
(2) Babu, Y. S.; Sack, J. S.; Greenhough, T. J.; Bugg, C. E.; Means, A. R.; Cook, W. J. *Nature* **1985**, *315*, 37−40.
(3) Chattopadhyaya, R.; Meador, W. E.; Means, A. R.; Quiocho, F. A. *J. Mol. Biol.* **1992**, *228*, 1177−1192.
(4) Kuboniwa, H.; Tjandra, N.; Grzesiek, S.; Ren, H.; Klee, C. B.; Bax, A. *Nat. Struct. Biol.* **1995**, *2*, 768−776.
(5) Crivici, A.; Ikura, M. *Annu. Rev. Biophys. Biomol. Struct.* **1995**, *24*, 85−116.
(6) Jaren, O. R.; Kranz, J. K.; Sorensen, B. R.; Wand, A. J.; Shea, M. A. *Biochemistry* **2002**, *41*, 14158−14166.
(7) Zhang, M.; Tanaka, T.; Ikura, M. *Nat. Struct. Biol.* **1995**, *2*, 758−767.
(8) Vetter, S. W.; Leclerc, E. *Eur. J. Biochem.* **2003**, *270*, 404−414.
(9) Barbato, G.; Ikura, M.; Kay, L. E.; Pastor, R. W.; Bax, A. *Biochemistry* **1992**, *31*, 5269−5278.
(10) Tjandra, N.; Kuboniwa, H.; Ren, H.; Bax, A. *Eur. J. Biochem.* **1995**, *230*, 1014−1024.
(11) Baber, J. L.; Szabo, A.; Tjandra, N. *J. Am. Chem. Soc.* **2001**, *123*, 3953−3959.
(12) Yao, Y.; Schoeneich, C.; Squier, T. C. *Biochemistry* **1994**, *33*, 7797−7810.
(13) Evenas, J.; Forsen, S.; Malmendal, A.; Akke, M. *J. Mol. Biol.* **1999**, *289*, 603−617.
(14) Malmendal, A.; Evenas, J.; Forsen, S.; Akke, M. *J. Mol. Biol.* **1999**, *293*, 883−899.
(15) Johnson, J. D.; Snyder, C.; Walsh, M.; Flynn, M. *J. Biol. Chem.* **1996**, *271*, 761−767.
(16) Kasturi, R.; Vasulka, C.; Johnson, J. D. *J. Biol. Chem.* **1993**, *268*, 7958−7964.
(17) Peersen, O. B.; Madsen, T. S.; Falke, J. J. *Protein Sci.* **1997**, *6*, 794−807.
(18) Török, K.; Tzortzopoulos, A.; Grabarek, Z.; Best, S. L.; Thorogate, R. *Biochemistry* **2001**, *40*, 14878−14890.
(19) Yang, C.; Jas, G. S.; Kuczera, K. *J. Biomol. Struct. Dyn.* **2001**, *19*, 247−271.
(20) Fallon, J. L.; Quiocho, F. A. *Structure* **2003**, *11*, 1303−1307.

(21) Chang, S.-L.; Szabo, A.; Tjandra, N. *J. Am. Chem. Soc.* **2003**, *125*, 11379−11384.
(22) Wilson, M. A.; Brunger, A. T. *J. Mol. Biol.* **2000**, *301*, 1237−1256.
(23) Moerner, W. E.; Orrit, M. *Science* **1999**, *283*, 1670−1676.
(24) Xie, X. S.; Trautman, J. K. *Annu. Rev. Phys. Chem.* **1998**, *49*, 441−480.
(25) Stryer, L.; Haugland, R. P. *Proc. Natl. Acad. Sci. U.S.A.* **1967**, *58*, 719−726.
(26) Selvin, P. R. *Methods Enzymol.* **1995**, *246*, 300−335.
(27) Ha, T.; Ting, A. Y.; Liang, J.; Caldwell, W. B.; Deniz, A. A.; Chemla, D. S.; Schultz, P. G.; Weiss, S. *Proc. Natl. Acad. Sci. U.S.A.* **1999**, *96*, 893−898.
(28) Ha, T.; Zhuang, X.; Kim, H. D.; Orr, J. W.; Williamson, J. R.; Chu, S. *Proc. Natl. Acad. Sci. U.S.A.* **1999**, *96*, 9077−9082.
(29) Jia, Y.; Talaga, D. S.; Lau, W. L.; Lu, H. S. M.; DeGrado, W. F.; Hochstrasser, R. M. *Chem. Phys.* **1999**, *247*, 69−83.
(30) Deniz, A. A.; Laurence, T. A.; Beligere, G. S.; Dahan, M.; Martin, A. B.; Chemla, D. S.; Dawson, P. E.; Schultz, P. G.; Weiss, S. *Proc. Natl. Acad. Sci. U.S.A.* **2000**, *97*, 5179−5184.
(31) Chen, Y.; Hu, D.; Vorpagel, E. R.; Lu, H. P. *J. Phys. Chem. B* **2003**, *107*, 7947−7956.
(32) Dietrich, A.; Buschmann, V.; Muller, C.; Sauer, M. *Rev. Mol. Biotechnol.* **2002**, *82*, 211−231.
(33) Schuler, B.; Lipman, E. A.; Eaton, W. A. *Nature* **2003**, *421*, 94.
(34) Margittai, M.; Widengren, J.; Schweinberger, E.; Schroeder, G. F.; Felekyan, S.; Haustein, E.; Koenig, M.; Fasshauer, D.; Grubmueller, H.; Jahn, R.; Seidel, C. A. M. *Proc. Natl. Acad. Sci. U.S.A.* **2003**, *100*, 15516−15521.
(35) Brasselet, S.; Peterman, E. J. G.; Miyawaki, A.; Moerner, W. E. *J. Phys. Chem. B* **2000**, *104*, 3676−3682.
(36) Magde, D.; Elson, E. L.; Webb, W. W. *Biopolymers* **1974**, *13*, 29−61.
(37) Aragon, S. R.; Pecora, R. *J. Chem. Phys.* **1976**, *64*, 1791−1803.
(38) Nie, S.; Chiu, D. T.; Zare, R. N. *Anal. Chem.* **1995**, *67*, 2849−2857.
(39) Widengren, J.; Rigler, R.; Mets, U. *J. Fluoresc.* **1994**, *4*, 255−258.
(40) Meissner, O.; Haeberlein, H. *Biochemistry* **2003**, *42*, 1667−1672.
(41) Widengren, J.; Schwille, P. *J. Phys. Chem. A* **2000**, *104*, 6416−6428.
(42) Ying, L.; Wallace, M. I.; Balasubramanian, S.; Klenerman, D. *J. Phys. Chem. B* **2000**, *104*, 5171−5178.
(43) Eid, J. S. Ph.D. Thesis, University of Illinois at Urbana-Champaign, 2002.
(44) Allen, M. W.; Urbauer, R. J. B.; Zaidi, A.; Williams, T. D.; Urbauer, J. L.; Johnson, C. K. *Anal. Biochem.* **2004**, *325*, 273−284.
(45) Hemsley, A.; Arnheim, N.; Toney, M. D.; Cortopassi, G.; Galas, D. J. *Nucleic Acids Res.* **1989**, *17*, 6545−6551.
(46) Weiner, M. P.; Costa, G. L.; Schoettlin, W.; Cline, J.; Mauther, E.; Bauer, J. C. *Gene* **1994**, *151*, 119−123.
(47) Widengren, J.; Mets, U.; Rigler, R. *J. Phys. Chem.* **1995**, *99*, 13368−13379.
(48) Lakowicz, J. R. *Principles of Fluorescence Spectroscopy*, 2nd ed.; Kluwer Academic/Plenum: New York, 1999.
(49) Harms, G. S.; Pauls, S. W.; Hedstrom, J. F.; Johnson, C. K. *J. Fluoresc.* **1997**, *7*, 273−281.
(50) Johnson, M. L.; Faunt, L. M. *Methods Enzymol.* **1992**, *210*, 1−37.
(51) Swaminathan, R.; Krishnamoorthy, G.; Periasamy, N. *Biophys. J.* **1994**, *67*, 2013−2023.
(52) Luby-Phelps, K.; Lanni, F.; Taylor, D. L. *J. Cell. Biol.* **1985**, *101*, 1245−1256.
(53) Dedman, J. R.; Potter, J. D.; Jackson, R. L.; Johnson, J. D.; Means, A. R. *J. Biol. Chem.* **1977**, *252*, 8415−8422.
(54) Yang, C.; Kuczera, K. *J. Biomol. Struct. Dyn.* **2002**, *19*, 801−819.
(55) Maiti, S.; Haupts, U.; Webb, W. W. *Proc. Natl. Acad. Sci. U.S.A.* **1997**, *94*, 11753−11757.
(56) Schwille, P.; Kummer, S.; Heikal, A. A.; Moerner, W. E.; Webb, W. W. *Proc. Natl. Acad. Sci. U.S.A.* **2000**, *97*, 151−156.
(57) Coles, B. A.; Compton, R. G. *J. Electroanal. Chem. Interfacial Electrochem.* **1983**, *144*, 87−98.
(58) Daly, P. J.; Page, D. J.; Compton, R. G. *Anal. Chem.* **1983**, *55*, 1191−1192.
(59) Rigler, R.; Mets, U.; Widengren, J.; Kask, P. *Eur. Biophys. J.* **1993**, *22*, 169−175.
(60) Osborne, M. A.; Balasubramanian, S.; Furey, W. S.; Klenerman, D. *J. Phys. Chem. B* **1998**, *102*, 3160−3167.
(61) Hess, S. T.; Webb, W. W. *Biophys. J.* **2002**, *83*, 2300−2317.
(62) Ha, T.; Ting, A. Y.; Liang, J.; Deniz, A. A.; Chemla, D. S.; Schultz, P. G.; Weiss, S. *Chem. Phys.* **1999**, *247*, 107−118.
(63) Kim, S. A.; Heinze, K. G.; Waxham, M. N.; Schwille, P. *Proc. Natl. Acad. Sci. U.S.A.* **2004**, *101*, 105−110.
(64) Kohl, T.; Heinze, K. G.; Kuhlemann, R.; Koltermann, A.; Schwille, P. *Proc. Natl. Acad. Sci. U.S.A.* **2002**, *99*, 12161−12166.
(65) Schwille, P.; Meyer-Almes, F.-J.; Rigler, R. *Biophys. J.* **1997**, *72*, 1878−1886.
(66) Evenas, J.; Malmendal, A.; Thulin, E.; Carlstrom, G.; Forsen, S. *Biochemistry* **1998**, *37*, 13744−13754.
(67) Evenas, J.; Thulin, E.; Malmendal, A.; Forsen, S.; Carlstrom, G. *Biochemistry* **1997**, *36*, 3448−3457.
(68) Bayley, P.; Ahlstroem, P.; Martin, S. R.; Forsen, S. *Biochem. Biophys. Res. Commun.* **1984**, *120*, 185−191.
(69) Talaga, D. S.; Lau, W. L.; Roder, H.; Tang, J.; Jia, Y.; DeGrado, W. F.; Hochstrasser, R. M. *Proc. Natl. Acad. Sci. U.S.A.* **2000**, *97*, 13021−13026.
(70) Grunwell, J. R.; Glass, J. L.; Lacoste, T. D.; Deniz, A. A.; Chemla, D. S.; Schultz, P. G. *J. Am. Chem. Soc.* **2001**, *123*, 4295−4303.
(71) Kinosita, K. K. S., Jr.; Ikegami, A. *Biophys. J.* **1977**, *20*, 289−305.
(72) Haas, E.; Ephraim-Katchalski-Katzir; Steinberg, I. Z. *Biochemistry* **1978**, *17*, 5064−5070.
(73) Rothwell, P. J.; Berger, S.; Kensch, O.; Felekyan, S.; Antonik, M.; Wohrl, B. M.; Restle, T.; Goody, R. S.; Seidel, C. A. M. *Proc. Natl. Acad. Sci. U.S.A.* **2003**, *100*, 1655−1660.
(74) Heidorn, D. B.; Trewhella, J. *Biochemistry* **1988**, *27*, 909−915.
(75) Seaton, B. A.; Head, J. F.; Engelman, D. M.; Richards, F. M. *Biochemistry* **1985**, *24*, 6740−6743.
(76) Van der Meer, B. W. *Rev. Mol. Biotechnol.* **2002**, *82*, 181−196.
(77) James, L. C.; Tawfik, D. S. *Trends Biochem. Sci.* **2003**, *28*, 361−368.